

Experimental Verification of Dynamic Properties of a Hollow Aluminum Beam

Mert Bilir^{ID}, Muhsin Karakaş^{ID}, Akın Oktav*^{ID}, Emre Özdemir^{ID}, Ahmet Selim Savi^{ID}, Fatih Sevinç^{ID}, Hasan Ali Türkan^{ID}

Alanya Alaaddin Keykubat University, Rafet Kayış Faculty of Engineering Department of Mechanical Engineering, Antalya, Türkiye.

*akin.oktav@alanya.edu.tr

Abstract

In this study, analytical and computational analyses are performed to determine the dynamic properties of an aluminum hollow beam, and an experimental analysis is also performed. The experimental model is taken as a reference model and the computational model is updated accordingly using model updating tools. The damping behavior inherent in all physical structures is measured experimentally. According to the results of the cross-correlation modal assurance criterion, the experimental and computational results match well. The average error between the computational and experimental results for the first five damped natural frequency values is 1.5%.

Keywords: Hollow beam, Damping, Model update, Frequency response function.

Alüminyum Kutu Kesitli Kirişin Dinamik Özelliklerinin Deneysel Olarak Doğrulanması

Özet

Bu çalışmada, alüminyum boşluklu kirişin dinamik özelliklerini belirlemek için analitik ve hesaplamalı analizler gerçekleştirilmiş ve ayrıca deneysel bir analiz yapılmıştır. Deneysel model referans model olarak alınmış ve model güncelleme araçları kullanılarak hesaplamalı model buna göre güncellenmiştir. Tüm fiziksel yapılarda doğal olarak mevcut olan sönümlenme davranışı deneysel olarak ölçülmüştür. Çapraz korelasyon modal güvence kriteri sonuçlarına göre, deneysel ve hesaplamalı sonuçlar iyi bir şekilde eşleşmektedir. İlk beş sönümlü doğal frekans değeri için hesaplamalı ve deneysel sonuçlar arasındaki ortalama hata 1,5% olarak hesaplanmıştır.

Anahtar Kelimeler: Kutu kesitli kiriş, Sönümlenme, Model güncelleme, Frekans cevap fonksiyonu.

1. INTRODUCTION

Aluminum beams are used in many industries such as aerospace, automotive, defense, construction, and various industrial products. In the automotive industry, many load-bearing components of a body-in-white have properties similar to hollow beams [1, 2]. Automotive components are stimulated by internal and external influences that can cause fatigue, fracture, and damage. Dynamically induced vibrations can cause unwanted acoustic emissions [3]. Vibration analysis of an airplane wing is one of the critical problems during the design of the wing [4]. The vibration behavior of beams, which are components of various structures, is part of the dynamic characteristics of systems [5]. Hollow beams are also used in the defense industry. For example, tank barrels are composed of multiple hollow beams.

Hollow beams are often used in engineering structures because they are cheaper, lighter and easier to assemble. The main goals when creating new designs are to use lighter structures and increase strength. In addition to weight savings, material savings also provide a significant economic advantage. In a study, analytical and computational modal analysis procedures were applied on a hollow Euler-Bernoulli beam using Matlab and Ansys [6]. The researchers concluded that the error between the computational and analytical results decreases as the slenderness ratio of the hollow beam increases. They used the finite element method (FEM) to perform dynamic analysis on hollow cantilever beams of various diameters and compared their findings with analytical results. Another study reported a good agreement between Ansys Workbench results and theoretical results [7]. In the study, the researchers compared the natural frequencies of hollow and solid beams of circular cross-sections made of different materials using Ansys Workbench. They found that when the inner diameter of the circular beam is reduced, the transverse natural frequency values increase. The researchers also showed a way to determine the natural frequencies and mode shapes of a beam using a combined analytical and numerical method [8]. They concluded that it is better than the conventional finite element method considering the computational cost. In another research, an analytical modal analysis of aluminum and steel beams was performed.

The researchers performed a modal analysis of the cantilever beam using Euler-Bernoulli beam theory and calculated the natural frequencies and mode shapes using FEM [9]. The theoretical and experimental results were compared, and very close values were obtained [10]. In their study, the researchers obtained and compared the results of dynamic analysis of steel, aluminum, and fiberglass cantilever beams by performing analytical and experimental calculations using Ansys. By comparing the error rates, they concluded that the error is less at low frequencies than at high frequencies [11]. Researchers are trying to reduce the severity of vibrations that cause component wear and fatigue in vehicles. The severity of vibration problems increases when the mass of the vehicle is reduced. An aluminum cantilever beam was studied for the vibration reduction frame. Friction strips were used to reduce vibration, reduce the overall mass of the structure, and regulate the vibration amplitude [3]. In the study, the researchers presented the natural frequency variation of the beams to quantify the damage, the damaged area, and the magnitude of the damage [12]. As a result of the experiments and calculations, the damaged areas were accurately estimated.

In the relevant literature, it is observed that analytical and computational studies on hollow beams have been carried out, but studies on model updating and damping behaviors of the structures are limited. The model updating procedure is necessary not only for validation but also to complement the model in terms of damping properties. In this study, analytical and computational analyses are performed to determine the dynamic properties of an aluminum hollow beam, and an experimental analysis is also performed. The experimental model is taken as a reference model and the computational model is updated accordingly using the model update tools available in Siemens Simcenter3D v2022.2.

2. MATERIAL AND METHOD

The dynamic characterization study for the hollow aluminum beam is conducted using experimental and computational modal analysis procedures. The finite element model is a deterministic numerical solution model that facilitates the solution of complex problems in engineering fields [13]. The computational analysis is conducted using Simcenter 3D. In the work, a 750 mm × 20 mm × 10 mm hollow beam with a 2 mm wall thickness is used (Figure 1). The material is Aluminum 6063. The mechanical properties of the material are tabulated in Table 1. Four different methods were applied throughout the study. In Section 2.1, the first five undamped natural frequencies are calculated analytically using the Euler-Bernoulli beam equation. In Section 2.2, the structure is modeled in 2D and 3D using FEM, and the first five natural frequencies and associated mode shapes are calculated. In addition, these procedures are also performed using Matlab. Information about the experimental studies and results is given in Section 2.3. In Section 2.4, a model update analysis is performed based on the experimental results.

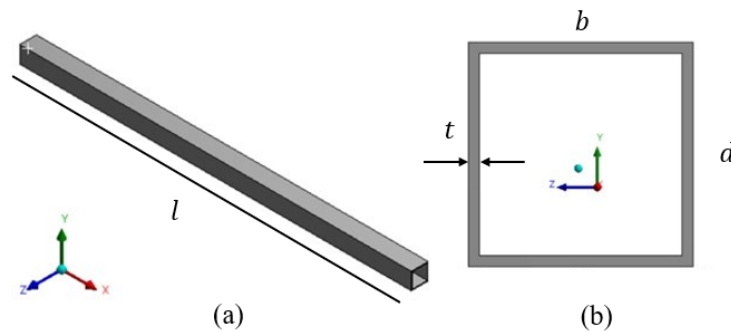


Figure 1. Dimensions of the cantilever beam (a) isometric view of the beam, (b) cross-section

Table 1. The dimensions and material properties of the Aluminum 6063 hollow beam

Parameter	Value
E : Young's modulus (GPa)	68.9
ν : Poisson's ratio	0.33
ρ : Density(kg/m ³)	2,755.4
l : Length (mm)	750
b : Width (mm)	20
d : Height (mm)	10
t : Wall thickness (mm)	2

2.1 Analytical Calculations

The equation of motion for isotropic cantilever uniform Euler-Bernoulli beam exposed to free vibration is given as [14-16]:

$$c^2 \frac{\partial^4 w}{\partial x^4}(x, t) + \frac{\partial^2 w}{\partial t^2}(x, t) = 0 \tag{1}$$

where w is the transverse deflection, and c is

$$c = \sqrt{\frac{EI}{\rho A}} \quad (2)$$

where E is Young's modulus, I is the area moment of inertia, ω is the circular frequency A is the cross-sectional area. The initial lateral displacement and velocity are taken as zero. Four boundary conditions for the cantilever beam are applied. The frequency equation and mode shape equation are given in Equation 3 and Equation 4, respectively.

$$\cos \beta_n l \cdot \cosh \beta_n l = -1 \quad (3)$$

$$W_n(x) = C_n[\sin \beta_n x - \sinh \beta_n x - \alpha_n(\cos \beta_n x - \cosh \beta_n x)] \quad (4)$$

where

$$\alpha_n = \left(\frac{\sin \beta_n l + \sinh \beta_n l}{\cos \beta_n l + \cosh \beta_n l} \right) \quad (5)$$

The natural frequency of the cantilever beam can be calculated by

$$\omega = \beta^2 \sqrt{\frac{EI}{\rho A}} \quad (6)$$

The values of $\beta_n l$ for the first five modes are 1.875, 4.694, 7.855, 10.996 and 14.137. Using Equation 6, the first 5 natural frequencies are calculated, and the values are tabulated in Table 2.

Table 2. The first five natural frequencies of the hollow beam calculated analytically (in Hz)

ω_1	ω_2	ω_3	ω_4	ω_5
18.1	113.5	317.9	622.9	1029.6

2.2 Computational Analysis (FEM)

For the computational analysis of the hollow beam, FEM is implemented in both Matlab and Simcenter 3D. For the studies carried out in Matlab; first, the physical properties and the number of elements are assigned. Mass and stiffness matrices are written (Equations 7 and 8). Discrete and continuous solutions are performed in Matlab. For the discrete solution, the number of elements is taken as 150, which means that the element size is 5 mm. The stiffness and mass matrices for the discrete solution are

$$[K] = \frac{EI}{l^3} \begin{bmatrix} 12 & 6l & -12 & 6l \\ 6l & 4l^2 & -6l & 2l^2 \\ -12 & -6l & 12 & -6l \\ 6l & 2l^2 & -6l & 4l^2 \end{bmatrix} \quad (7)$$

$$[M] = \frac{\rho A l}{420} \begin{bmatrix} 156 & 22l & 54 & -13l \\ 22l & 4l^2 & 13l & -3l^2 \\ 54 & 13l & 156 & -22l \\ -13l & -3l^2 & -22l & 4l^2 \end{bmatrix} \quad (8)$$

The eigenvalues and eigenvectors are computed using the $[V, D] = \text{eig}(K, M)$ command for the continuous solution. The mode shapes are plotted in Matlab, and the first five mode shapes are shown in Figure 2. The mode shapes shown are obtained only for transverse deflection.

The calculations made so far have been done both discretely and continuously using Matlab. In continuous solution the number of degrees of freedom is infinite. Eigenvectors and eigenvalues are used for continuous solutions. In the discrete solution, the number of degrees of freedom is finite. In the discrete solution, the finite element method is used, and the discrete solution is performed by assigning stiffness and mass matrix equations.

To construct the FE model in Simcenter 3D, the element type, material properties, mesh structure, and boundary conditions must be provided. First, geometry is drawn, and a mesh structure is formed on the CAD. Afterwards, the material information is assigned. Then, 2D and 3D modeling are performed using all these steps, and the results are compared and interpreted.

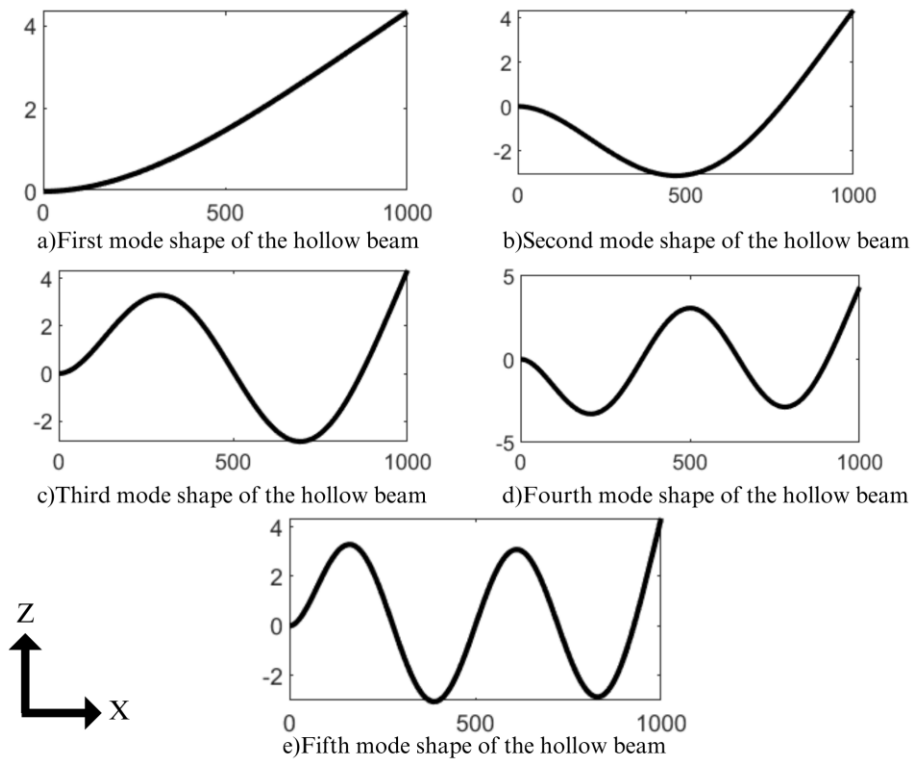


Figure 2. The first five mode shapes of the hollow beam

For 2D modeling, the midsurface of the hollow beam is extracted. Then, since the material is isotropic, the wall thickness value of the midsurface is assigned. A mesh structure is created using CQUAD 4 type four-node, two-dimensional elements. The element size for the hollow beam starts at 9 mm and is decreased until convergence in the results is achieved. Natural frequency values are determined with the Nastran SOL103 solver. Natural frequency values converge at 5 mm element size. Cantilever beam boundary conditions are used in the analysis. Additional boundary conditions are also specified for only the transverse movement of the beam.

For 3D modeling, the entire volume of the model is used, and the mesh structure is created with CHEXA8 eight-node elements. 2D mesh model results and 3D mesh model results are expected to be slightly different because the 2D mesh model considers only a flat surface, while the 3D mesh model considers the whole volume. 3D mesh models are known to be more accurate for complex geometries because they automatically form mid-nodes which take into account certain motions such as rotation and bending in the element level.

After the computational modal analysis in FEM, the accelerometer locations need to be determined for the experimental modal analysis. The accelerometer locations shown in Figure 3 are based on the computational modal analysis solution performed in Simcenter 3D software. A mesh size of 5 mm is used to determine the accelerometer locations. The maximum distance between accelerometers is determined to be 20 mm. Eight locations have been identified and one of these locations is for excitation. The distance between the nodes is measured in the software based on the fixed point for the placement of the accelerometers during the experiment. Moreover, the software shows not only the position of the accelerometers but also the angle of placement of the accelerometers. Figure 3 shows the sensor positions and angles determined by the software.

In Table 3, the calculation results for both 2D mesh and 3D mesh and Matlab results are tabulated for comparison. For FEM, mesh size is very important for processing time. To reduce processing time, the convergence of the results should be taken as a basis and the convergence should be used for the operations. The convergence value can be easily found by checking the convergence graph. The autocorrelation matrix shown in Figure 4 is a measure of the degree of correlation between two mode shapes of the same mode shape set. The results revealed a perfect correlation which means that the computation performed to determine the optimal sensor locations is successful. The diagonal matrix values are perfectly 1 and all off-diagonal terms are well below 0.1.

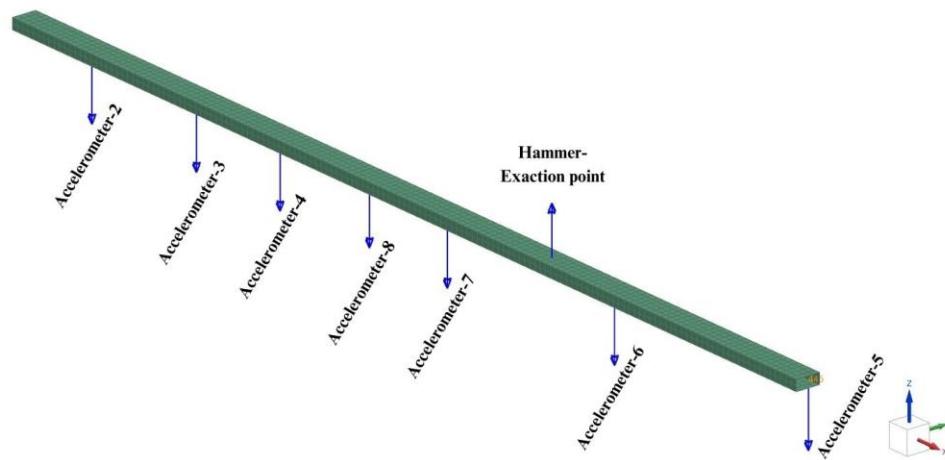


Figure 3. The optimal accelerometer locations and the optimal excitation location computed by the algorithm built-in Simcenter 3D.

Table 3. The first five natural frequencies of hollow beam obtained by different types of analysis

	Size	ω_1	ω_2	ω_3	ω_4	ω_5
Computational 2D	5 mm	18.8 Hz	117.3 Hz	326.1 Hz	632.1 Hz	1031.0 Hz
Computational 3D	5 mm	19.2 Hz	120.2 Hz	334.8 Hz	650.9 Hz	1065.0 Hz
Matlab calculations	Discrete (5mm)	18.1 Hz	113.5 Hz	317.8 Hz	622.9 Hz	1029.6 Hz
	Continuous	18.1 Hz	113.5 Hz	317.9Hz	622.9 Hz	1029.6 Hz

In the study, 2D and 3D convergence graphs are examined, and it is seen that the analysis results are very close since the experimental subject does not have a complex geometry. Therefore, the ideal mesh size is chosen as 5 mm. If the structure used had a larger and more complex geometry, the analysis results would

have shown more significant differences and consequently, the mesh size chosen would have changed accordingly.

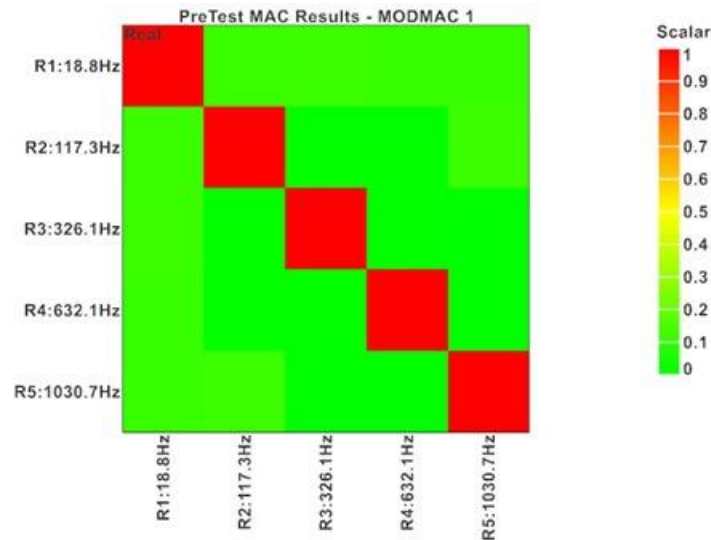


Figure 4. The autocorrelation matrix

2.3 Experimental Analysis

The hollow aluminum beam is fixed to the fixture at one end to provide a fixed-free boundary condition. An eight-channel Sinus™ mobile analyzer is used for data acquisition and recording. 7 Dytran™ uniaxial accelerometers are employed for the measurements. Accelerometers are used to transfer the acceleration signals caused by hammer strikes, i.e., the response of the structure to the analyzer. The specific accelerometer brand used in the experiment is Dytran 3035BG. Seven accelerometers were used simultaneously in the experiment. The beam is excited with an impact hammer, and an average of 3 impact measurements are recorded to be analyzed through the measurement software, Samurai. The roving hammer used during the analysis is a Dytran 5800B3 with a sensitivity value of 48.70 mV/LbF.

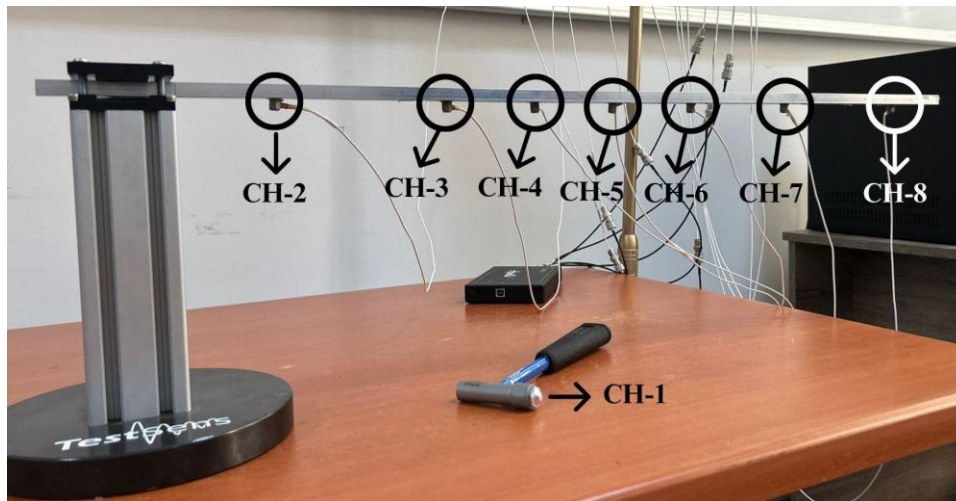


Figure 5. Experimental setup (Vibration & Acoustics Laboratory, Alanya Alaaddin Keykubat University)

The positions of the accelerometers and the location to be hit with the impact hammer were determined by an algorithm in Simcenter 3D. The locations and channel numbers are shown in Figure 5. In the mobile

analyzer, Channel#1 is reserved for the roving hammer, and other channels (#2 to #8) are employed for the accelerometers. The results are compared with FEM results and interpreted. Based on the results, the model is updated in Section 2.4.

The measurements are done to obtain the frequency response functions (FRFs), which are used to determine the natural frequencies, damping ratios and mode shapes of the engineering structures. After processing the raw data, the response can be obtained as displacement, velocity or acceleration [17].

The coherence function informs us about how well the measured data is in line with the actual response of the engineering structure and whether there are any detrimental effects in the data that affect the response i.e., nonlinearities, self-induced vibration, etc. In modal analysis, it is a measure of the correlation between the input excitation and the measured response. In the cantilever beam experiment, the resulting high coherence values indicate that the measured response is highly correlated with the excitation signal, and the measured data are reliable for postprocessing [18]. To give an idea, an FRF function and its coherence function obtained from Channel#6 are shown in Figure 6. The damped natural frequency values obtained during the experimental study are tabulated in Table 5. The mathematical relation between the undamped natural frequencies (ω_n) and the damped natural frequencies (ω_d) is

$$\omega_d = \omega_n \sqrt{1 - \zeta^2} \tag{9}$$

where ζ is the damping ratio.

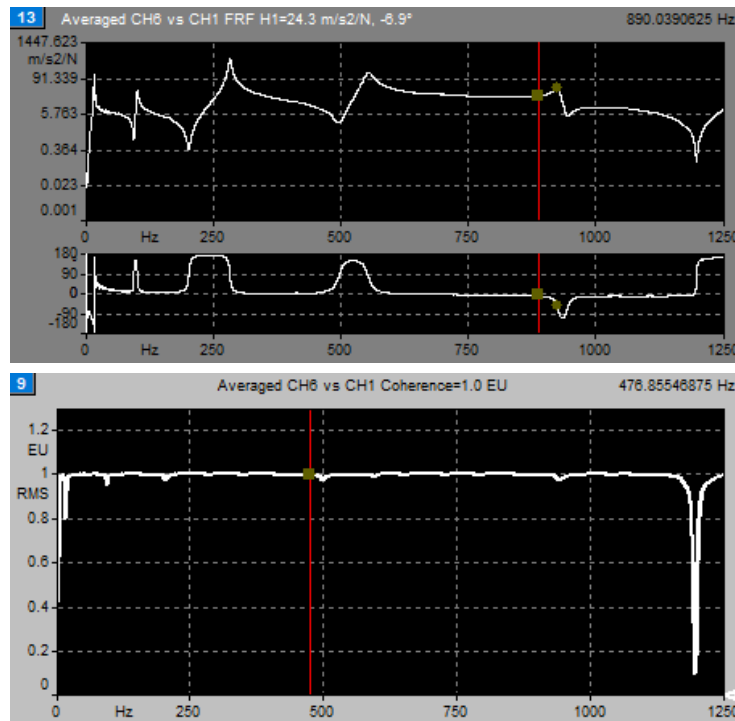


Figure 6. The FRF (top) and the coherence function (bottom) graphs obtained from Channel#6

Table 5. The first five natural frequencies of hollow beam obtained by the experimental modal analysis

ω_1	ω_2	ω_3	ω_4	ω_5
16.6 Hz	101.5 Hz	283.1 Hz	556.4 Hz	924.9 Hz

2.4 Model Update

The data acquired from the experimental modal analysis study is compared with the results of the computational modal analysis. The experimental data is taken as reference data and the computational model is updated to minimize the difference between the two models. The mode shapes are compared using the modal assurance criterion (MAC). It is observed that the mode shapes are similar, but the frequency values associated with the mode shapes are slightly different. The reason is that the natural frequency values (ω_n) obtained from the computational analysis are undamped, while the values obtained from the experimental modal analysis are the damped natural frequencies (ω_d). The damping ratio (ζ) is measured during the experiments to be included in the computational model. MAC compares the mode shapes in two sets of modes and indicates the degree of consistency between the shapes. The MAC is computed using the following equation:

$$\text{MAC}(A_k, A_l) = \frac{|\sum_{j=1}^N \Psi_{Akj} \Psi_{Alj}^*|^2}{\sum_{j=1}^N \Psi_{Akj} \Psi_{Akj}^* \sum_{j=1}^N \Psi_{Alj} \Psi_{Alj}^*} \quad (10)$$

where Ψ_{Akj} and Ψ_{Alj} are the j th value of the mode shape vectors $\{\Psi_{Ak}\}$ and $\{\Psi_{Al}\}$, respectively. First, 7 accelerometers are placed on the FE model obtained from Simcenter 3D for the analysis using nCode. The positions of the accelerometers are the same as in the experimental setup. The positions and measurement directions of the accelerometers on the hollow beam are shown in Figure 7.

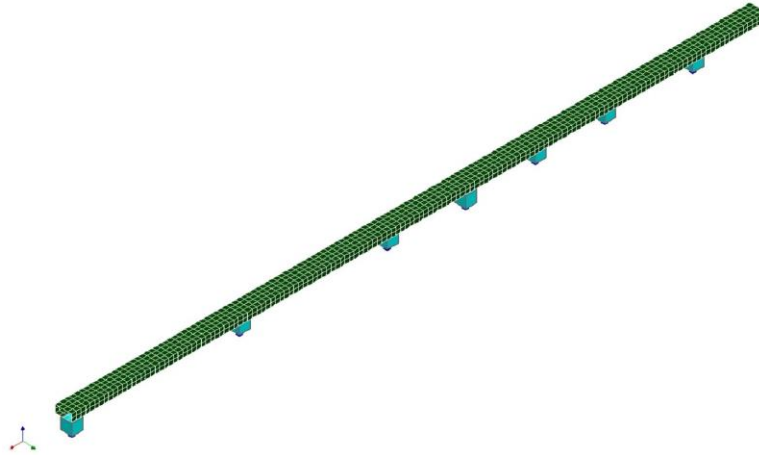


Figure 7. Positions of the accelerometers on the hollow beam (nCode analysis)

Then, using nCode software, a MAC analysis is performed to compare the first 5 mode shapes obtained from the computational analysis results. The first 5 experimental mode shapes are generated in nCode. A comparison of the computational and experimental mode shapes is given in the next subsection.

3. COMPARISON OF RESULTS

Analytical, experimental, and computational results are obtained throughout the study. The analytical calculations do not consider damping, which is inherent in all physical systems. The initial computational model also does not include damping. The damping was measured experimentally using FRFs and incorporated into the updated model by adding viscous damping elements. The viscous damping elements added to the updated computational model are shown in Figure 8. The 1D viscous damping elements are assigned a damping value of 0.32 N·s/mm (shown in orange in Figure 8).

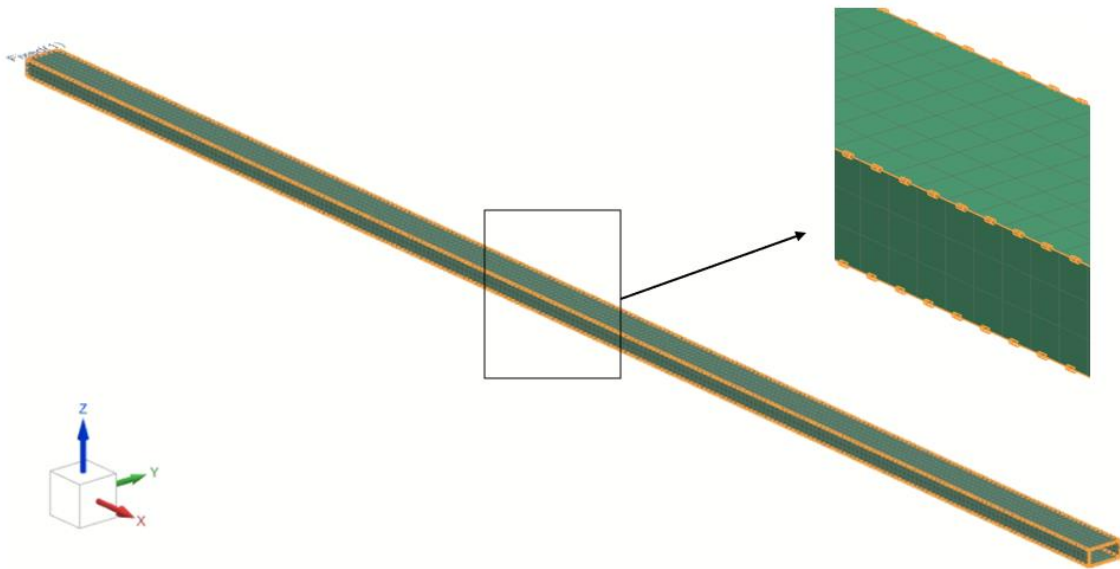


Figure 8. Viscous damping elements introduced the updated computational model (shown in orange)

Table 5. The first five mode frequencies of the hollow beam obtained by the analytical, computational and experimental analysis (in Hz)

Analysis	ω_1	ω_2	ω_3	ω_4	ω_5
Analytical	18.1	113.5	317.9	622.9	1,029.6
Matlab (discrete solution)	18.1	113.5	317.9	622.9	1,029.6
Computational (initial model)	18.8	117.4	326.3	632.4	1,031.0
Experimental	16.6	101.5	283.1	556.4	924.9
Computational (updated model)	17.1	100.2	285.1	559.2	906.0

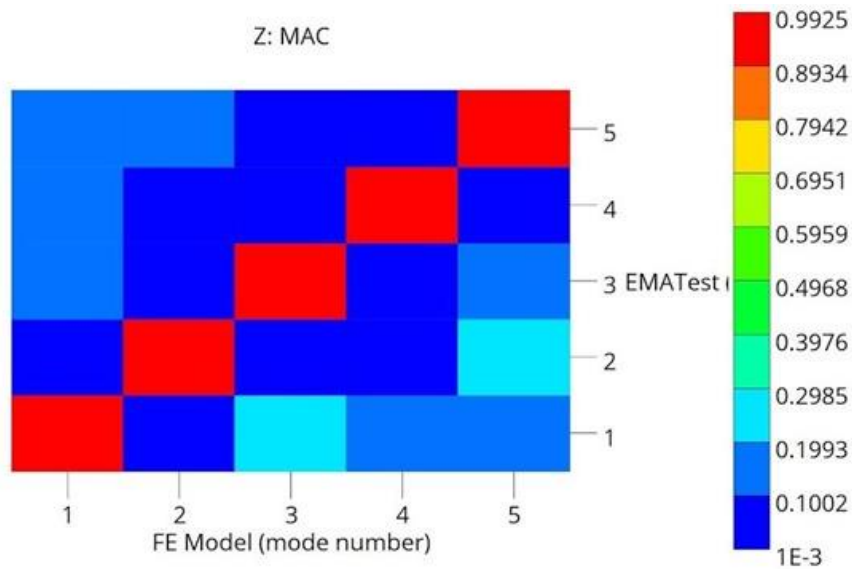


Figure 9. Cross-correlation of MAC matrix: comparison of experimental and computational mode shapes

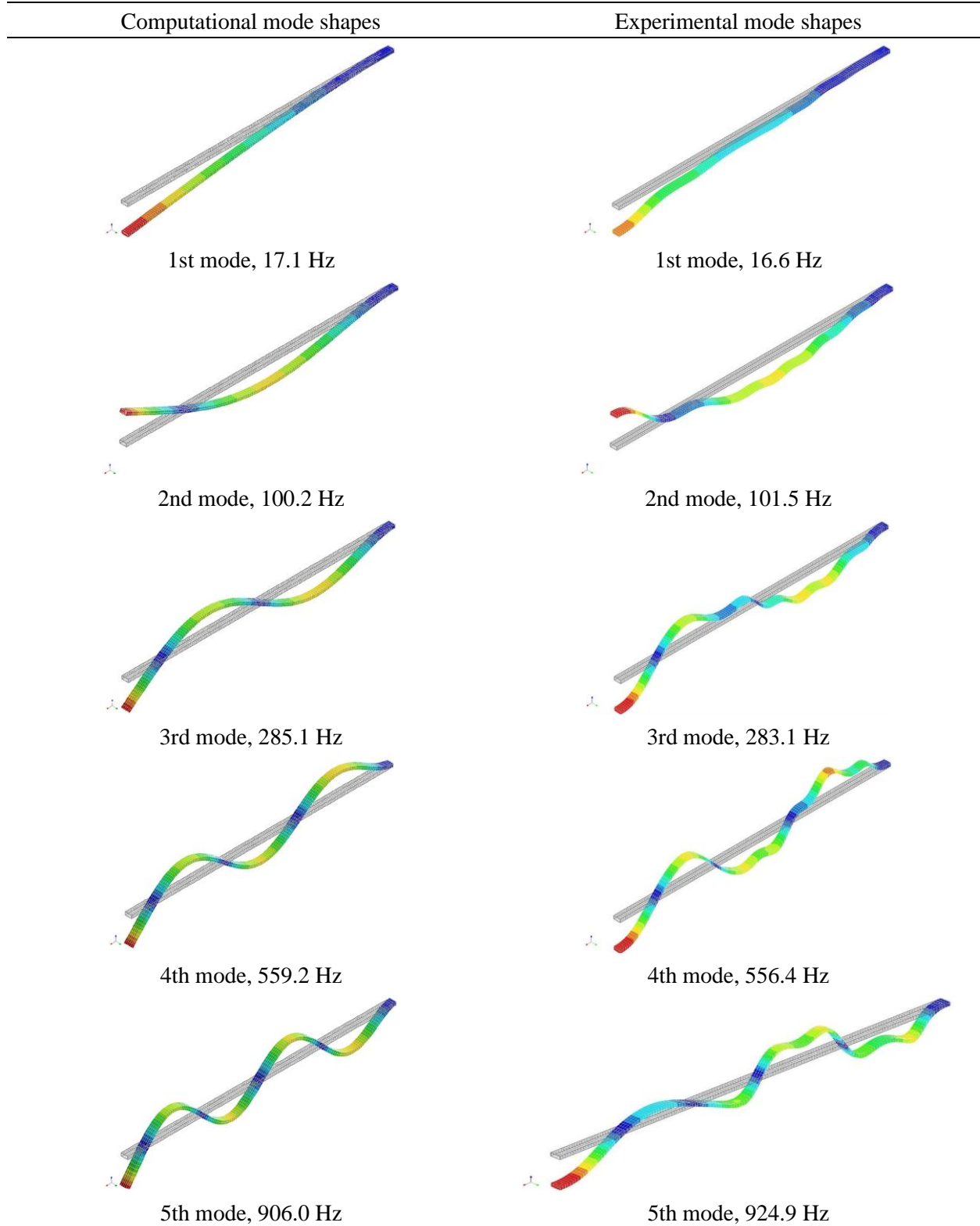


Figure 10. Computational (left column) and experimental (right column) mode shapes

The results tabulated in Table 5 show that the updated computational model is the model that best fits the experimental results in terms of mode frequencies. The cross-correlation MAC matrix compares the computationally and experimentally derived eigenvectors (aka mode shapes). The color scale in Figure 9 represents correlation values ranging from 0 to 1. As the value approaches 1, the similarity increases and as the value approaches 0, the similarity decreases. As a result of the study, values close to 1 are obtained in the diagonally positioned cross-correlation MAC matrix. This diagonal arrangement can be interpreted as a successful completion of the conducted analysis. The experimental and computational mode shapes are compared in Figure 10.

4. CONCLUSION

Structural parameter estimation is affected by uncertainties which are present in the system. The relevant literature reveals the importance of model updating. A technique is proposed to estimate spatially distributed parameters of samples with regular geometry structure using Karhunen Loève expansion and sensitivity based FRF model updating [19]. A model updating study is performed on an H-cross section steel beam [20]. The model is updated using natural frequencies measured in an impact hammer test of the beam structure and the validity of the updated model is confirmed by the strain responses measured from the test. In a recent study, several model updating methods based on full-scale model tests of track beams are compared [21]. The results of a model update study on a composite beam show that the uncertainties in the simulated finite element model like the modulus of elasticity of the fibers and matrices, individual densities, modulus of rigidity, and most importantly the fiber orientations can be effectively corrected by using direct updating method [22].

In this study, the dynamic properties of an aluminum hollow beam are investigated using analytical, computational, and experimental methods. An analytical solution is carried out according to the assumptions of the Euler-Bernoulli beam theory. The assumptions of the theory negatively affect the accuracy of the results as the frequency range increases. Discrete and continuous solutions for the structure are realized using Matlab. The number of elements is taken as 150 for the discrete Matlab solution and infinite for the continuous solution. The tabulated results in Table 5 show that the analytical and Matlab solutions overestimate the mode frequencies compared to the experimental results.

The initial computational model, which does not consider damping, also overestimates the results. The computational model is updated regarding the experimental model. The damping behavior inherent in all physical structures is measured experimentally and added to the updated computational model. It is then observed that the experimental and computational results match well. The average error between the computational and experimental results for the first five damped natural frequency values is calculated to be 1.5%. In line with the former studies [19-22], this study shows the importance of model updating for correct analysis and design. Differently, in this study, damping elements were also taken into account which refines and improves the results in terms of suppressing the errors between the experimental and computational results.

5. ACKNOWLEDGEMENT

This research was supported by The Scientific and Technological Research Council of Turkey (TUBITAK), 2209A Program, Project number: 1919B012220892.

REFERENCES

- [1] Zannon, M. (2014). Free vibration of thin film cantilever beam. *International Journal of Engineering and Technical Research (IJETR)*, 2, 304-314.

- [2] Piranda, J., Corn, S., Bouhaddi, N., Stawicki, C., Van Herpe, F., & Cudney, H. H. (1998, February). Determination of equivalent beam properties for hollow girders typically used in the automotive industry. In *Society for Experimental Mechanics, Inc, 16 th International Modal Analysis Conference*. (Vol. 2, pp. 1227-1232).
- [3] Machhan, R. A., & Könke, C. (2021). Investigation of different types of damping effects for automotive components—preliminary work. *Materials Today: Proceedings*, 46, 9659-9666.
- [4] Demirtaş, A., & Bayraktar, M. (2019). Free vibration analysis of an aircraft wing by considering as a cantilever beam. *Selçuk Üniversitesi Mühendislik, Bilim Ve Teknoloji Dergisi*, 7(1), 12-21.
- [5] Chaphalkar, S. P., Khetre, S. N., & Meshram, A. M. (2015). Modal analysis of cantilever beam structure using finite element analysis and experimental analysis. *American Journal of Engineering Research*, 4(10), 178-185.
- [6] İnan, C. Y., & Oktav, A. (2021). Model Updating of a Euler-Bernoulli Beam Using the Response Method. *Kocaeli Journal of Science and Engineering*, 4(1), 16-23.
- [7] Flaieh, E. H., Dwech, A. A., & Mosheer, M. R. (2021, February). Modal analysis of fixed-free beam considering different geometric parameters and materials. In *IOP Conference Series: Materials Science and Engineering* (Vol. 1094, No. 1, p. 012118). IOP Publishing.
- [8] Wu, J. S., & Chou, H. M. (1998). Free vibration analysis of a cantilever beam carrying any number of elastically mounted point masses with the analytical-and-numerical-combined method. *Journal of Sound and Vibration*, 213(2), 317-332.
- [9] Prashant, S. W., Chougule, V. N., & Mitra, A. C. (2015). Investigation on modal parameters of rectangular cantilever beam using experimental modal analysis. *Materials Today: Proceedings*, 2(4-5), 2121-2130.
- [10] Imran, M., Abbasi, A. A., & Hyder, M. J. (2016, October). Determination of modal characteristics of cantilever beam. In *2016 International Conference on Emerging Technologies (ICET)* (pp. 1-3). IEEE.
- [11] Mokalke, G. C., & Sutar, A. V. (2016). Modal analysis of cantilever beam for various cases and its analytical and FEA analysis. *International Journal of Engineering Technology, Management and Applied Sciences*, 4(2), 60-66.
- [12] Jassim, Z. A., Ali, N. N., Mustapha, F., & Jalil, N. A. (2013). A review on the vibration analysis for a damage occurrence of a cantilever beam. *Engineering Failure Analysis*, 31, 442-461.
- [13] Korucu, S., Gök K., Tümsük, M., Soy, G., & Gök, A. (2019). Farklı profillere sahip kirişlerde meydana gelen eğilme gerilmesi ve sehim miktarının teorik ve nümerik yöntemler ile analizi. *Dokuz Eylül Üniversitesi Mühendislik Fakültesi Fen ve Mühendislik Dergisi*, 21(62), 469-482.
- [14] Inman, D.J., *Engineering Vibration*. 3rd ed. 2007, New Jersey: Prentice Hall.
- [15] Timoshenko, S. P., & Gere, J. M. (2009). *Theory of Elastic Stability*. Courier Corporation.
- [16] Young, D., & Felgar, R. P. (1949). Tables of characteristic functions representing normal modes of vibration of a beam. Bureau of Engineering Research.
- [17] Irvine, T. (2000). An introduction to frequency response functions. *Rapport, College of Engineering and Computer Science, 2000*.

- [18] Ewins, D. J. (2009). *Modal testing: theory, practice and application*. John Wiley & Sons.
- [19] Machado, M.R., Adhikari, S., Dos Santos, J.M.C. & Arruda, J.R.F. (2018). Estimation of beam material random field properties via sensitivity-based model updating using experimental frequency response functions. *Mechanical Systems and Signal Processing*, 102,180-197.
- [20] Oh, B. K., Kim, M. S., Kim, Y., Cho, T., & Park, H. S. (2015). Model updating technique based on modal participation factors for beam structures. *Computer-Aided Civil and Infrastructure Engineering*, 30(9), 733-747.
- [21] Zhong, J., Gou, H., Zhao, H., Zhao, T., & Wang, X. (2022, January). Comparison of several model updating methods based on full-scale model test of track beam. *Structures*, 35, 46-54.
- [22] Bagha, A. K., Gupta, P., & Panwar, V. (2020). Finite element model updating of a composite material beam using direct updating method. *Materials Today: Proceedings*, 27, 1947-1950.